

# Enhancement of Solar Farm Connectivity with Smart PV Inverter PV-STATCOM

Rajiv K. Varma, *Senior Member, IEEE*, Ehsan M. Siavashi, *Member, IEEE*

**Abstract**—This paper presents an innovative smart PV inverter control as STATCOM (PV-STATCOM) for obviating the need for a physically connected STATCOM in a distribution network for controlling steady state voltage and temporary over voltages (TOVs) resulting from unsymmetrical faults. Two 10 MW PV solar systems are already connected in the distribution feeder of a utility in Ontario, Canada. A STATCOM is installed to prevent the steady-state voltage and TOV issues arising from the connection of a third 10 MW PV solar farm at same bus. It is demonstrated from PSCAD electromagnetic transient studies that if the proposed PV-STATCOM control is implemented on the incoming third 10 MW PV solar farm, all the above voltage issues are mitigated satisfactorily as required by the utility Grid Code. This proposed smart inverter PV-STATCOM control therefore eliminates the need for the physical STATCOM, saving an enormous cost for utilities dealing with voltage rise and TOV issues with grid connected PV systems. Such a control can effectively increase the Distributed Generator hosting capacity of distribution feeders at more than an order of magnitude lower cost under similar network conditions. Moreover, this novel grid support functionality can open new revenue making opportunities for PV solar farms.

**Index Terms**— Photovoltaic Solar system, Smart Inverter, PV-STATCOM, Voltage Control, Reactive Power Control, Temporary Over Voltage, FACTS

## I. INTRODUCTION

Distributed Generators (DGs) bring several benefits to distribution networks. However, these benefits come along with new challenges [1]-[2]. Some of these challenges include steady state overvoltage, temporary overvoltage (TOV), unbalanced voltage, power quality issues such as harmonics, frequent operation of conventional voltage regulators such as load tap changers and capacitor banks, changes in feeder power factor, etc [1]-[5]. High penetration of solar farms is known to cause reverse power flows resulting in over voltages at PCC which potentially limit any future DG installations [6]-[7]. Traditionally, shunt capacitor banks (SCs), on-load tap changers (OLTC) and step type voltage regulators (SVRs) are utilized for voltage control in the distribution systems [8]. However, these devices are slow acting with a response time ranging from seconds to few minutes. Moreover, these devices such as OLTC and SVR operate based on unidirectional flow of power and cannot operate reliably during bidirectional power flows caused by Distributed Generators e.g.

The financial support from Ontario Centres of Excellence (OCE) and Hydro One under the grants WE-SP109-E50712-08 and CR-SG30-11182-11; and that from NSERC are gratefully acknowledged. Rajiv K. Varma and Ehsan M. Siavashi are with the ECE Department, University of Western Ontario, London, Ontario, N6A 5B9, Canada (e-mail: rkvarma@uwo.ca; emohamm4@uwo.ca).

solar farms. Flexible AC Transmission Systems (FACTS) such as Static Var Compensator (SVC) and STATCOM are utilized in general for voltage regulation purposes in power systems [9]. These devices can provide voltage control with a response time of 1-3 cycles with STATCOM being much faster than SVC [9].

The Ontario Independent Electricity System Operator (IESO) proposed the installation of a -33/+48 Mvar Static Var Compensator (SVC) to provide the dynamic reactive power requirement of the 100 MW PV solar farm at the Grand Renewable Energy Park (GREP) in Haldimand County, Nanticoke, Ontario [10]. An SVC is proposed to prevent rise in customer voltage caused by interconnection of PV solar systems in a Japanese distribution feeder [11]. Small size STATCOMs are also proposed in Japan to mitigate voltage rise issues due to surplus power injected by PV solar farms in distribution feeders [8]. Studies for determining optimal size and location of SVC for improving voltage regulation at different operating conditions of residential PV solar systems connected in an Egyptian distribution feeder are described in [12]. A D-STATCOM is proposed to improve voltage regulation due to variability of power output from PV solar systems in an Australian distribution network [13].

Four STATCOMs in the range 1-2 Mvar have been actually installed in Massachusetts, USA, at various locations to mitigate feeder voltage rise and voltage fluctuations in a distribution feeder caused by variability of power output from a cluster of 13 MW PV solar systems [14]. A 6 Mvar STATCOM is installed at the substation of 52.5-megawatt (MW) Shams Ma'an PV solar project in Jordan to maintain a smooth voltage profile under different network conditions and variable PV output [15].

A case study of a 44 kV distribution feeder with two 10 MW PV solar farms is reported in [16]. Connection of a third 10 MW solar farm failed the power distance test of the utility indicating that voltage issues will be caused by its interconnection. Reconductoring the feeder to improve X/R ratio or relocation of the PCC of the solar farms to another feeder were considered to be economically unviable solutions. The utility decided to install a STATCOM for regulating the steady state voltage to within utility acceptable limits. It is noted that the conventional symmetrical voltage control provided by SVCs (and STATCOMs) worsen the problem of Temporary Overvoltages in an actual transmission system in California [17]. Hence a new unsymmetrical control is needed, which is considered in this paper.

Smart inverters have been proposed for PV solar systems to effectively counteract voltage issues [18-19]. Smart inverter functions such volt/var, volt/watt, off-unity power factor, Low/High Voltage Ride Through, Low/High Frequency Ride

Through and Dynamic Reactive Current Injection, etc. have been demonstrated in field applications [20-21]. Grid Codes such as IEEE 1547 have been revised in the interim [22]. The newly proposed smart inverter functions as described in the revised IEEE 1547 (2018) although provide ride through capability but not Temporary Overvoltage mitigation [22] explicitly.

A unique control of PV solar farms as STATCOM during nighttime for providing various grid support functions with full inverter capacity and for delivering the same benefits during daytime with PV inverter capacity remaining after real power generation was introduced in 2009 [23-24]. The proposed control, termed PV-STATCOM, was utilized for increasing the connectivity of wind farms [25] and for improving the power transmission capacity [26]. The above control however has a limitation of available reactive power capacity especially during noontime when the inverter is completely utilized for real power generation.

The control of PV solar farms as a smart inverter PV-STATCOM was proposed in [27]. The control presented in this paper provided only steady state voltage control in the grid by three-phase symmetrical real power generation by PV systems. However, the control strategy proposed in [27] cannot provide mitigation of Temporary Overvoltage (TOV) during unsymmetrical faults which is a major issue in the integration of PV solar farms. For suppressing TOV, an entirely different control is required, which is the main contribution of this paper.

This paper is based on a patent-pending technology for modulation of real and reactive power of PV solar farms [28]. Implementation of this control on a PV solar farm allows the solar farm to provide a 24/7 functionality as a STATCOM with rated inverter capacity both during nighttime and any time during the day as needed by the grid, including full-noon.

The novelty of this paper is that a new smart inverter PV-STATCOM solution is proposed for mitigating steady state voltage rise and more importantly Temporary Overvoltage caused by high penetration of PV solar systems. Traditionally, to address these issues, dynamic reactive power compensators such as Static Var Compensator (SVC) and STATCOM, have not only been proposed [8], [10-13] but actually installed in several parts of the world [14-16] including Canada and USA. In this paper, the effectiveness of the PV-STATCOM technology has been shown on a realistic distribution feeder in Ontario where an actual STATCOM has been installed for steady state voltage control [16]. It is demonstrated that the proposed PV-STATCOM can provide the same functionality of steady state voltage control and moreover provide TOV mitigation, thus eliminating the need of the installed STATCOM. The PV-STATCOM solution is highly cost-effective (about 50 times cheaper) compared to actual SVCs and STATCOMs as it utilizes the existing electrical substation infrastructure such as buswork, transformers, breakers, protection systems, of the PV solar system (which are quite similar to those in actual SVCs and STATCOM installations). The PV-STATCOM technology can therefore potentially bring significant cost-savings to utilities in that they may not need to install expensive SVCs or STATCOMs. Moreover, this novel grid support functionality can open new revenue making opportunities for PV solar farms.

This paper presents: a) control concept of the proposed PV-STATCOM, and b) EMTDC/PSCAD simulation of the PV-STATCOM technology on the third 10 MW PV solar inverter in [16] for steady state voltage control. The proposed PV-STATCOM control further provides mitigation of temporary over voltage (TOV) which is not considered in [16].

The remainder of this paper is organized as follows. Section II illustrates the concept of proposed smart PV inverter control as STATCOM. The study system is described in Section III. Section IV demonstrates the modeling of the study system. Section V explains the controller design process for the study system. The proposed control is validated through PSCAD/EMTDC software simulations in Section VI. Discussions are presented in Section VII while the conclusions are enunciated in Section VIII.

## II. CONCEPT OF SMART PV INVERTER CONTROL AS STATCOM

The real power generation from a solar farm on a sunny day and the remaining unutilized inverter capacity over a 24 hour period is depicted in Fig. 1. The operating modes of the proposed PV-STATCOM are described below:

i) Full PV mode: The PV solar farm operates at unity power factor with no reactive power control.

ii) Partial STATCOM Mode: The inverter capacity remaining after active power production is utilized for dynamic reactive power control as STATCOM.

ii) Full STATCOM mode: During a power system disturbance or fault in the day, when the need for reactive power support is high, the solar farm temporarily (for typically less than a minute) reduces its real power output to zero by varying the voltage across the solar panels. It further makes its entire inverter capacity available for dynamic reactive power control as STATCOM. After the grid support need is fulfilled, the solar farm returns to its pre-disturbance power output. The Full STATCOM mode can be activated at any time during the day depending upon system need. As an example, this Full-STATCOM mode is depicted by the thin rectangle around 8 am in Fig. 1. The width of the rectangle is less than a minute but is shown over an exaggerated time period of an hour, just for ease of understanding. This mode is also fully available during night.

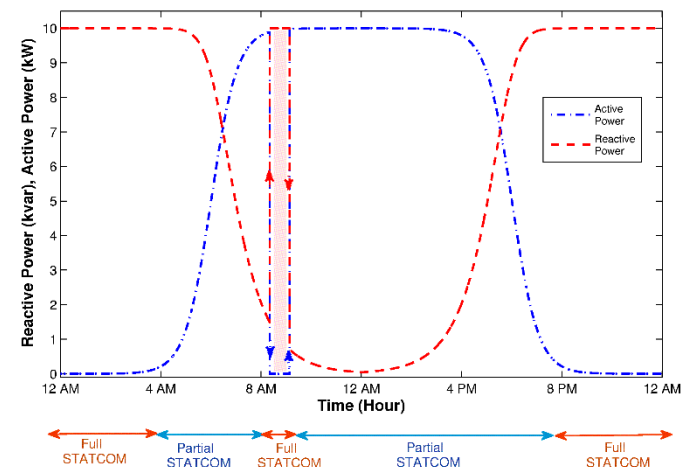


Fig. 1. Concept of smart PV inverter control as STATCOM (PV-STATCOM)

### III. STUDY SYSTEM

Fig. 2 shows a 44 kV feeder in a utility distribution network in Ontario, Canada (name and location withheld for confidentiality reasons) [16]. The study feeder system includes three 10 MW PV systems with a total capacity of 30 MW connected about 35 km away from the utility transformer station (TS). The 30 MW PV plants are connected to the distribution system through a 30 MVA interface transformer, although each 10 MW PV system uses an intermediate transformer prior the interface transformer. Two solar systems with 10 MW generation are already connected to the PCC. Connection of the additional 10 MW PV system causes increased reverse power flow during light load conditions resulting in steady state over voltages. A 3.5 Mvar STATCOM is installed at PCC to mitigate steady state overvoltages.

The TOV is also observed to exceed the permissible limits during single line to ground faults (SLGF) or line to line ground (L-L-G) fault scenarios.

According to an Ontario utility requirement [29] the TOV caused by a DG facility should be less than 1.25 p.u. and in no circumstance exceed 1.30 p.u.

### IV. MODELING OF THE STUDY SYSTEM

This section presents the modeling of different components of the study system in EMTDC/PSCAD software. The model of the study system is depicted in Fig. 3. The substation system is represented as an equivalent voltage source with 1.05 p.u. voltage to supply the 44 kV feeder. The 35 km line from substation to PCC is represented by a  $\pi$  model in which the shunt admittance (e.g. line charging) is neglected. In Fig. 3,  $R_g$  and  $L_g$  represent the line resistance and inductance, respectively. The electrical load is considered to be a constant-power static RL load. At nominal voltage of 44 kV<sub>L-L</sub>, the total load is considered to be 30 MVA. The peak-time active and reactive loads are considered to be 27 MW and 6 Mvar, respectively, whereas during off-peak hours, these loads are 6 MW and 1.5 Mvar, respectively.

All three PV systems are utilized with 10 MVA two-level six-pulse IGBT-based voltage source inverters (VSI). The switching frequency is chosen to be 4 kHz to minimize the switching losses. For each PV system, an LCL filter is utilized to mitigate the harmonics caused by the switching frequency. The LCL filter consists of a series inductor ( $L_f$ ), shunt capacitor ( $C_f$ ) with series damping resistor ( $R_d$ ) and another series inductor ( $L_t$ ) corresponding to the transformer inductance. The combination of shunt capacitor in series with damping resistor is connected in delta configuration. The filter inductor is selected between 0.1 to 0.25 pu [30]. The amount of reactive power generated by the filter capacitor also influences the reactive power compensation by the VSI. Hence, the filter capacitor value is designed to limit the reactive power exchange below 0.05 pu of the inverter power rate. To avoid resonance between filter capacitor and inductor, a damping resistor is added to filter capacitor in series [31].

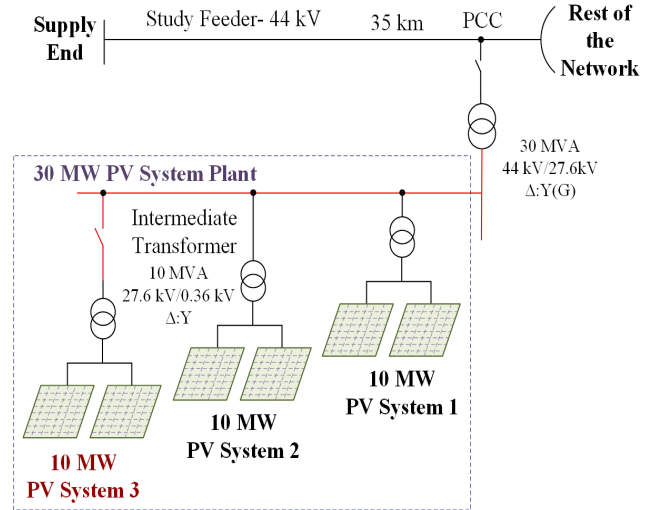


Fig. 2. Single line diagram of the study system

### V. CONTROLLER DESIGN

This paper proposes that the additional (third) 10 MW PV system be equipped with the proposed patent-pending smart PV inverter PV-STATCOM control [28]. The other two PV systems use only conventional controllers to generate real power at unity power factor.

Fig. 3 illustrates the schematic of the smart PV inverter controller. The controller is designed in  $d-q$  frame and includes  $abc/dq$  transformation block, PLL, DC controller, current controllers, AC voltage controller, TOV detector unit and PWM unit. The PLL unit extracts the phase angle of PCC voltage for transforming currents and voltages from  $abc$ -frame to  $dq$ -frame or vice versa [32]. The DC controller, in order to regulate DC link voltage at the reference value, generates the reference current for  $d$ -component of inverter current which represents the active current component. Consequently, the current controller in  $d$ -axis regulates the active current component to its reference value [32].

During daytime, the smart PV control operates as a conventional PV system i.e., in Full PV mode. If steady state voltage control is required in all three phases, together with real power generation, Partial STATCOM mode is activated. The Full STATCOM mode is activated when a temporary overvoltage TOV occurs due to unsymmetrical faults. MPPT based on incremental conductance method [30] is utilized during Full PV mode and Partial STATCOM mode. In Full-STATCOM mode, the MPPT mode is disabled and the real power generation is made zero by making the voltage across PV panel equal to its open circuit voltage. The entire inverter capacity is then utilized to absorb reactive power in order to reduce the phase voltage. After the TOV is mitigated, power production from the solar panels is enabled and control mode is switched to Partial STATCOM mode.

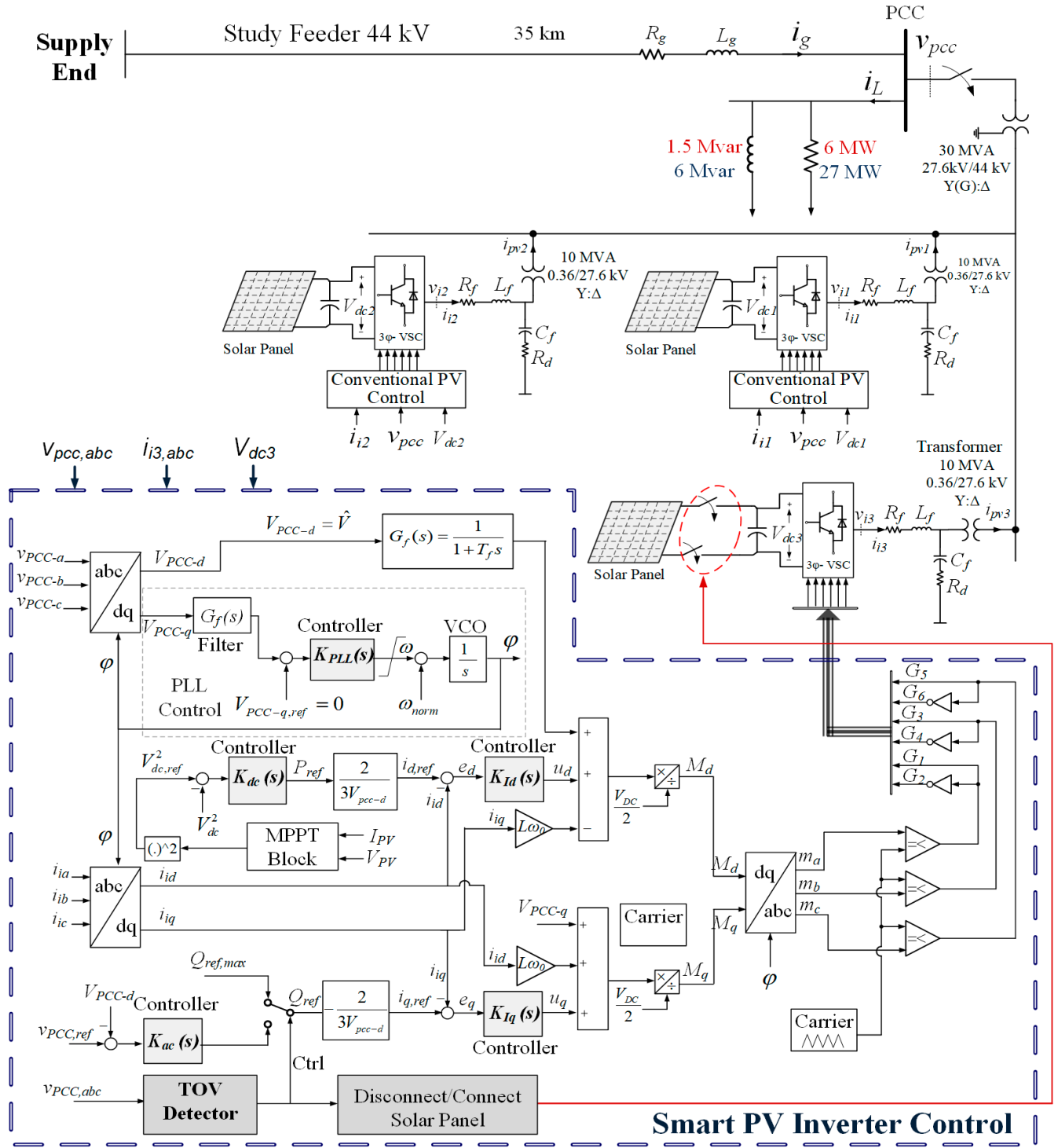


Fig. 3. Modeling of the study system and control components

The PCC voltage is controlled by the AC voltage controller. Therefore, either maximum reactive current or output of the AC voltage controller defines the reference value of reactive current control loop. The current controller in  $q$ -axis regulates the reactive current to its reference value. It is noted that the TOV Detector unit switches between voltage control mode and TOV mitigation mode. Also, this unit generates the command to enable or disable the power production from PV solar panels. The outputs of the controller are modulation indices in  $d$ - $q$

frame, which are eventually converted to  $abc$ -frame using the phase angle of PCC voltage. The modulation indices in  $abc$ -frame are compared with carrier signal to generate gate pulses for the VSC switches [30], [32].

#### A. Operation Mode Selector

Fig. 4 shows the flowchart of the smart PV inverter control to select the operation mode. During daytime, the voltages in three phases are measured. If any phase voltage exceeds the



TOV limit while the voltages in other phase/phases decrease substantially, the output of TOV Detector unit is triggered “ON”, and Full STATCOM mode is activated. The controller keeps the inverter current lagging the inverter voltage by 90 degrees (i.e. keeps absorbing reactive power) to reduce TOV until the phase voltages reach an acceptable value.

After the fault is cleared all the phase voltages will rise to their normal values. The controller thus recognizes that TOV is mitigated. It therefore enables power generation from the solar panels and switches to Partial STATCOM mode for steady-state voltage control. In partial STATCOM mode, the controller regulates the PCC voltage with  $Q_{rem}$ , which is the inverter capacity remaining after real power generation.

During nighttime, the PV solar system operates in Full STATCOM mode to control either the steady-state voltage or TOV. The smart PV inverter control thus autonomously determines its operation mode and prioritizes between active power generation and reactive power exchange based on the system requirements, nature of transient/disturbance, time of the day and remaining inverter capacity.

### B. Phase Locked Loop Control

The PCC voltage components in  $dq$ -frame are as:

$$V_{pcc-d} = \hat{V} \cos(\omega_0 t + \theta_0 - \varphi) \quad (1)$$

$$V_{pcc-q} = \hat{V} \sin(\omega_0 t + \theta_0 - \varphi) \quad (2)$$

$$\frac{d\varphi}{dt} = \omega(t) \quad (3)$$

where,  $\hat{V}$  is the amplitude of PCC phase voltage,  $\omega_0$  is system frequency and  $\theta_0$  is the initial phase angle of the AC system. By selecting  $\varphi_{ref} = \omega_0 t + \theta_0$ , the voltage components become  $V_{pcc-d} = \hat{V}$  and  $V_{pcc-q} = 0$ . Therefore, regulating  $V_{pcc-q}$  to zero by PLL control will lead to DC components in  $dq$ -frame [32]. In Fig. 3, to remove high frequency harmonics, a low pass filter with transfer function  $G_{filter}(s)$  and time constant  $T_f = 1 \text{ ms}$  is used after the transformation block.  $K_{pll}$  is the controller transfer function to regulate phase angle  $\varphi$  at  $\varphi_{ref} = \omega_0 t + \theta_0$ . The Voltage-Controlled Oscillator (VCO) block is a resettable integrator which converts frequency to phase angle. The equation for phase angle is given by:

$$\frac{d\varphi}{dt} = \hat{V} K_{pll} \mathcal{L}^{-1}(G_{filter}(s))(\varphi_{ref} - \varphi) \quad (4)$$

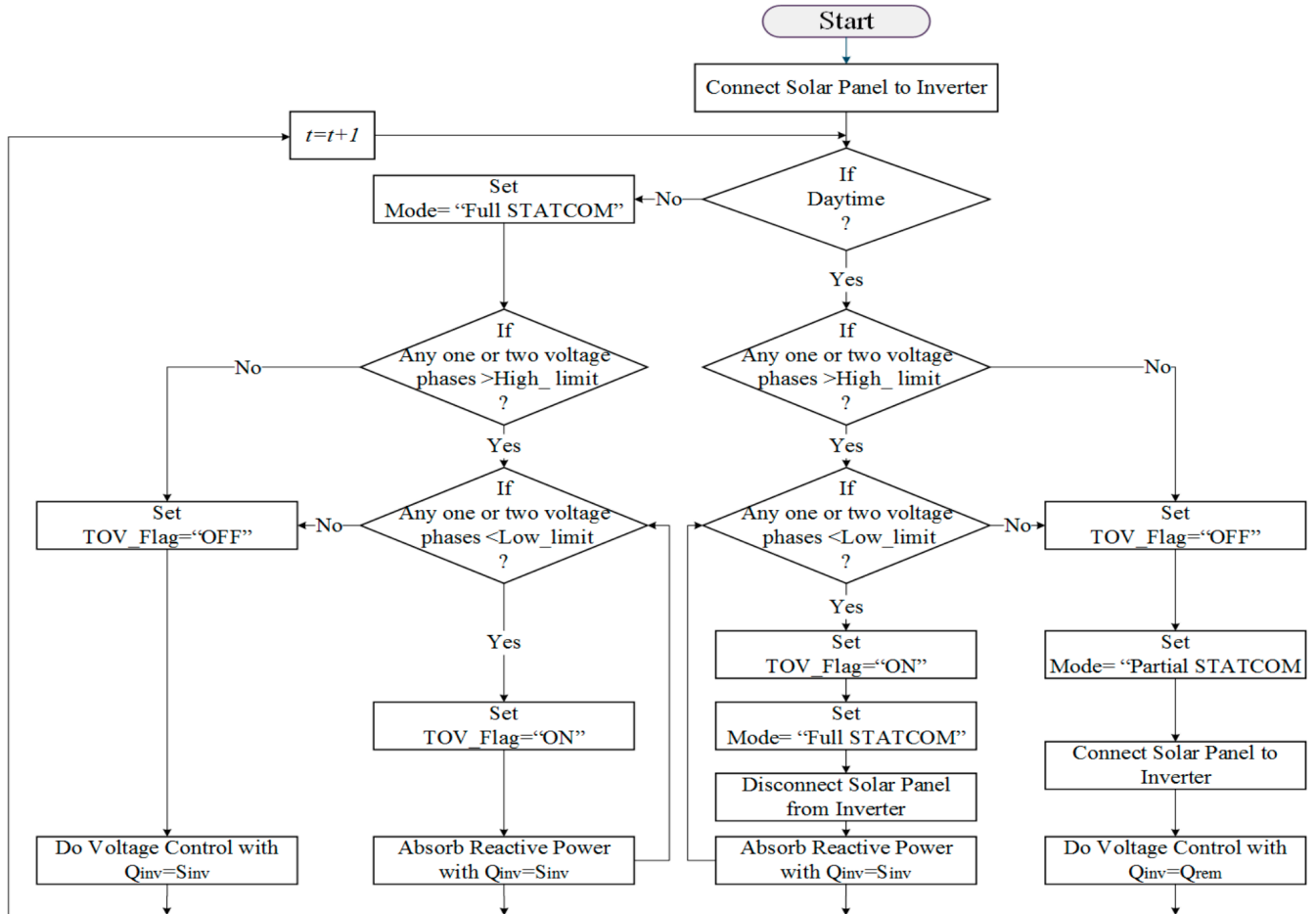


Fig.4. Flowchart of the smart PV inverter operating mode

It should be noted that  $(\omega_0 t + \theta_0 - \varphi)$  has a very small value. Hence, it can be assumed that  $\sin(\omega_0 t + \theta_0 - \varphi)$  is about equal to  $(\omega_0 t + \theta_0 - \varphi)$ . The open loop transfer function of PLL with PI controller is:

$$H_{PLL}(s) = K_{PLL}(s) \times G_{PLL}(s) = \frac{\hat{V} \times k_{PLL, gain}}{T_f} \left( \frac{s + z_{PLL}}{s + T_f^{-1}} \right) \frac{1}{s^2} \quad (5)$$

where  $k_{PLL, gain}$  and  $z_{PLL}$  are PLL controller parameters. The ‘‘Symmetrical Optimum’’ technique [33] is used to design the PI controller with phase margin  $\delta_m = 60^\circ$  at cross over frequency  $\omega_c = 268$  rad/s.

### C. Current Control

The active and reactive power outputs of the inverter in  $dq$ -frame are [32]:

$$P_i(t) = \frac{3}{2} (v_{id}(t) i_{id}(t) + v_{iq}(t) i_{iq}(t)) \quad (6)$$

$$Q_i(t) = \frac{3}{2} (-v_{id}(t) i_{iq}(t) + v_{iq}(t) i_{id}(t)) \quad (7)$$

Due to PLL operation  $v_{id} = \hat{V}$  and  $v_{iq} = 0$ . Therefore, the real power output of the inverter is controlled by  $i_{id}$  while reactive power output is controlled by  $i_{iq}$ . However, the references values of the current controllers are received from outer loops based on control objectives and operation mode.

The inverter currents in  $dq$ -frame are [32], [34]:

$$L_f \frac{di_{id}}{dt} = L_f \omega(t) i_{iq} - R_f i_{id} + \frac{V_{dc}}{2} M_d - V_{pcc-d} \quad (8)$$

$$L_f \frac{di_{iq}}{dt} = -L_f \omega(t) i_{id} - R_f i_{iq} + \frac{V_{dc}}{2} M_q - V_{pcc-q} \quad (9)$$

where  $V_{dc}$  is the DC link voltage,  $M_{dq}$  is modulation indices,  $V_{pcc, dq}$  are PCC voltages,  $i_{i, dq}$  are inverter currents and  $V_{i, dq}$  are the voltages at AC side of the inverter in  $dq$  frame, respectively. By adding feed-forward terms to the control signals, (8) and (9) are transformed to linear and decoupled equations.

$$L_f \frac{di_{id}}{dt} + R_f i_{id} = u_d \quad (10)$$

$$L_f \frac{di_{iq}}{dt} + R_f i_{iq} = u_q \quad (11)$$

where  $u_d$  and  $u_q$  are input control signals. Other terms of (8) and (9) are added to control signals to obtain the modulation indices. Modulation indices are transformed to  $abc$ -frame and in the final stage are compared with carrier signal to generate the IGBT gate pulses. Although, the dynamic equations of current in  $d$ - $q$  frame are stable, a  $PI$  controller is used to make the steady-state error zero and decrease the response time. To reduce the response time, the controller moves the transfer function pole farther from origin of the real-imaginary coordinates [26].

### D. DC Link Voltage Control

Due to losses in the switches of the inverter, the DC link of the inverter needs to absorb a slight amount of active power to maintain the DC voltage at the specific level. The required level of the DC voltage is determined by the AC side voltage of the inverter. When sun is available, the control utilizes a small amount of dc power from the solar panels to keep the capacitor charged, while the rest of the solar power is injected into the grid. During Full STATCOM mode or during nighttime, the inverter control absorbs a small amount of real power from the grid and charges the capacitor through inverter diodes. In Fig. 3, the power balance at DC side is as follows [34]:

$$P_{PV} = P_{dc-cap} + P_{dc} \quad (12)$$

where  $P_{PV}$ ,  $P_{dc-cap}$  and  $P_{dc}$  are PV panel power, DC-link capacitor power and DC side power of the VSC. By ignoring the VSC loss and filter losses, the DC side power of VSC can be considered equal to the power on the AC side. Hence,

$$P_{dc} = P_i = \frac{3}{2} v_{id} i_{id} \quad (13)$$

$$P_{dc-cap} = \frac{d}{dt} \left( \frac{1}{2} C V_{dc}^2 \right) \quad (14)$$

$$P_{PV} = n_p I_{sc} V_{dc} - n_p I_0 V_{dc} \left[ e^{\left( \frac{q V_{dc}}{k T n_s} \right)} - 1 \right] \quad (15)$$

where,  $I_0$  is the diode saturation current, electron charge  $q = 1.6e^{-19}$  coulomb,  $T$  is the cell temperature,  $k = 1.38e^{-23}$  is the Boltzmann’s constant, while  $n_s$  and  $n_p$  are the number of series and parallel cells. Due to non-linearity in the equation for solar power generation, the solar power is added as a feed-forward term to offset its effect [35]. The closed loop transfer function of  $d$ -component of invert current is given as:

$$G_{id}(s) = \frac{i_{id}(s)}{i_{id, ref}(s)} \quad (16)$$

Thus,

$$\frac{C}{2} \frac{d}{dt} (V_{dc}^2) = P_{PV} - \frac{3}{2} v_{id} \mathcal{L}^{-1}(G_{id}(s)) i_{id, ref} \quad (17)$$

Fig. 5 demonstrates the block diagram of the DC link voltage control based on (17). The open loop transfer function of DC link voltage control with PI controller is:

$$H_{dc}(s) = K_{dc}(s) \times G_{dc}(s) = - \frac{3 \times V_{pcc-d} \times k_{dc, gain}}{2 \times \sigma_{i, d}} \left( \frac{s + z_{dc}}{s + \sigma_{i, d}^{-1}} \right) \frac{1}{s^2} \quad (18)$$

where  $k_{dc, gain}$  and  $z_{dc}$  are the parameters of DC link voltage controller. Symmetrical Optimum technique [33] is used to design this controller with phase margin  $\delta_m = 50^\circ$  at cross over frequency  $\omega_c = 364$  rad/s.

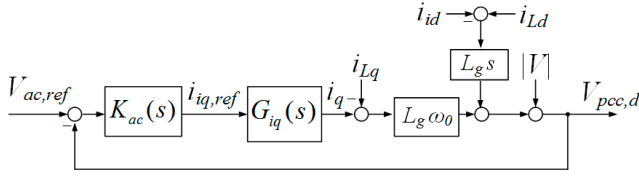


Fig. 6. Block diagram of AC-bus voltage controller

### E. PCC Voltage Control

In voltage control mode, the AC voltage controller defines the reactive current reference for current controller. However, in TOV reduction mode the reference value for reactive current controller is set to the maximum value as determined from the inverter kVA/MVA rating. This done to reduce the TOV in the most effective manner with largest possible inductive current. From Fig. 3, the PCC voltage is [32], [34]:

$$V_{pcc-d} = -L_g \omega_0 i_{gq} + L_g \frac{di_{gd}}{dt} + \hat{V} \quad (19)$$

$$V_{pcc-q} = L_g \omega_0 i_{gd} + L_g \frac{di_{gq}}{dt} \quad (20)$$

where  $i_{g,dq}$  are  $d$ - $q$  axis grid currents and  $L_g$  is grid inductance. It is noted that  $V_{pcc-q}$  is controlled at zero level by PLL controller, and so,  $V_{pcc-d}$  represents the PCC voltage. By neglecting the current of the shunt filter capacitor,

$$i_{g,dq} = i_{L,dq} - i_{i,dq} \quad (21)$$

where,  $i_{L,dq}$  are load current components in  $d$ - $q$  frame. Therefore, the PCC voltage is expressed as:

$$V_{pcc-d} = -L_g \omega_0 i_{iq} + L_g \omega_0 i_{Lq} - L_g \frac{di_{id}}{dt} + L_g \frac{di_{Ld}}{dt} + \hat{V} \quad (22)$$

The voltage control loop generates the reference for the reactive component of the inverter current control. The outer voltage

control loop needs to be slower than inner current control loop [24]. Fig. 6 shows the AC link voltage control based on (20). By using an Integral controller, the open loop transfer function of the PCC voltage is expressed as:

$$H_{ac}(s) = \frac{k_{gain,ac}}{s} \times G_{iq}(s) \times (-L_g \omega_0) = \frac{-L_g \omega_0 k_{gain,ac}}{s(1 + \sigma_{i,q} s)} \quad (23)$$

It should be noted that other terms of (22) are added as feed-forward terms.

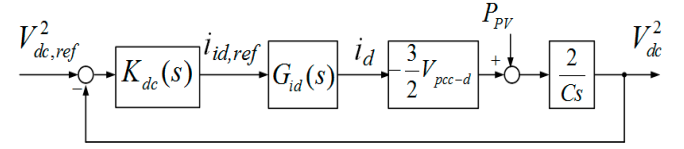


Fig. 5. Block diagram of DC-bus voltage controller

### F. TOV Detection Block

The TOV Detection block triggers the TOV flag when a temporary overvoltage occurs. When TOV flag is “ON”, the controller transforms the PV system into the Full STATCOM mode by changing the DC voltage to the open circuit voltage level of the solar panels thereby virtually disconnecting the solar panels. Reactive power is then absorbed using the full inverter capacity. When the fault is cleared and PCC voltage has reached acceptable value, the TOV flag is triggered “OFF” and the smart PV controller transforms into the Partial STATCOM mode for voltage control.

Fig. 7 depicts the structure of the TOV Detection block. This block includes three different sections, Voltage Rise Detection (VRD), Voltage Fall Detection (VFD) and Fault Detection (FD) units. Each unit uses rms blocks to obtain the rms value of each phase and then converts it to its per-unit value. The Voltage

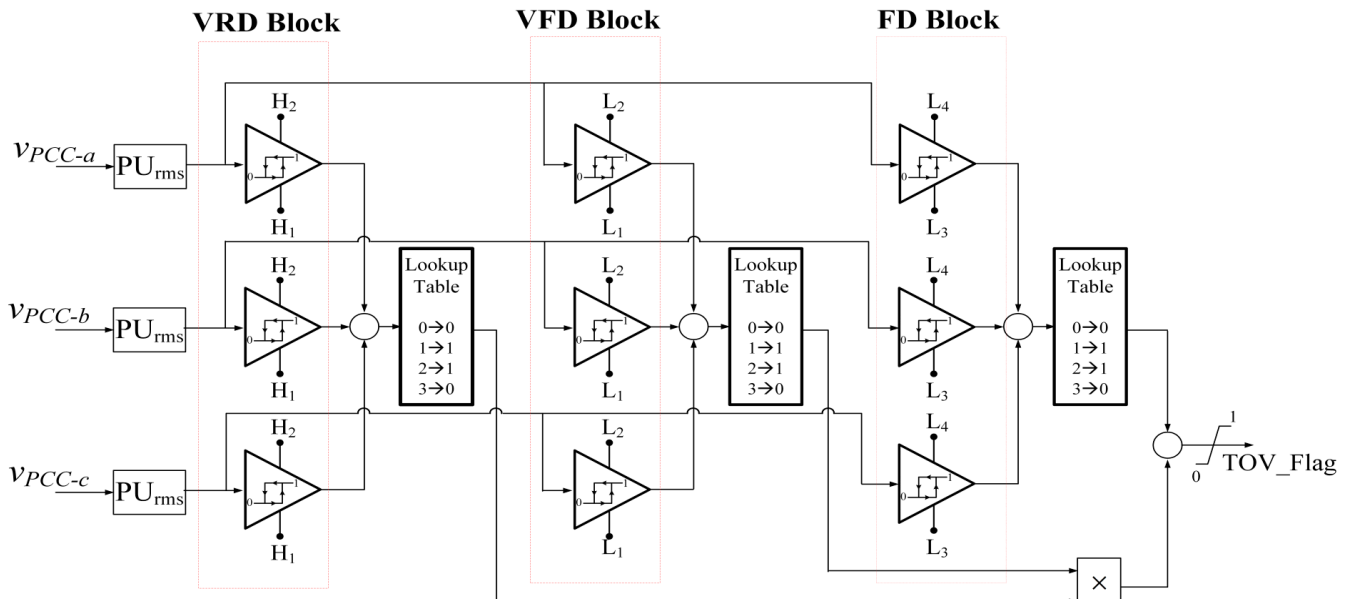


Fig. 7. Structure of TOV Detection block

Rise Detection unit compares the per-unit voltage of each phase with its hysteresis band limits. If one or two of the phase voltages exceed the high band limit, the output of VRD unit is set to “1” otherwise the output is “0”. Based on the Ontario grid connection requirements, the low and high band limits of the hysteresis block for VRD unit are chosen as 1.20 pu and 1.25 pu, respectively. The VFD unit detects the fall in voltage. The output of VFD is triggered to “1” if one or two phase voltages pass the lower limit of the hysteresis band. The low and high bands of VFD unit are 0.8 pu and 0.85 pu respectively. When the output of both VRD and VFD blocks are “1” the TOV Detection block recognizes the TOV event and triggers the output to “1”. In other words, the TOV event is detected when one or two phase voltages are larger than 1.25 pu and voltages of other phase/phases are below 0.8 pu. After the fault is cleared all phase voltages will be above a certain value which is chosen as 0.85 pu.

Hence, FD unit triggers the TOV flag to become “0” when the fault is cleared. The Look Up Table in each case operates such that it provides a True “1” signal if the desired condition is met only in either one or two phases, but will give a False “0” output if the desired condition is met on all or none of the three phases. The hysteresis limits for different units are as below:

$$\begin{cases} \text{VRD unit} \rightarrow H_1 = 1.20 \text{ pu}, H_2 = 1.25 \text{ pu} \\ \text{VFD unit} \rightarrow L_1 = 0.80 \text{ pu}, L_2 = 0.85 \text{ pu} \\ \text{FD unit} \rightarrow L_3 = 0.50 \text{ pu}, L_4 = 0.55 \text{ pu} \end{cases} \quad (24)$$

## VI. PSCAD/EMTDC SIMULATION STUDIES

The performance of the smart PV inverter PV-STATCOM while fulfilling two control objectives, voltage control and TOV reduction, are presented in this section. The PSCAD/EMTDC software is used for the simulation of the study system shown in Fig. 3. In all these studies, light (small) load is defined as 6 MW and 2 Mvar, whereas a heavy (large) load is considered to be 27 MW and 9 Mvar. All the three solar farms are considered to be producing 7 MW each during light load conditions, i.e., a total of 21 MW power.

### A. Conventional PV System without Smart Inverter Control

In this study, the incoming third 10 MW PV solar system does not have a smart PV inverter control. It operates as a conventional PV solar system with real power generation at unity power. Fig. 7 illustrates the PCC voltages in the three phases and their per-unit rms values when PV systems generate their rated power during small load conditions.

Before connection of PV systems, the PCC voltage is about 1.04 pu which is in the acceptable range per code [29]. However, after the connection of the PV systems, the voltage rises to 1.10 pu which is unacceptable [29].

At  $t = 0.54$  sec a single line-to-ground (SLG) fault is initiated on phase “A”. This causes the voltage of phase “A” to fall to zero whereas the voltages in the other two phases reach 1.35 pu during the fault. This temporary overvoltage (TOV) during SLG fault is beyond the utility specified limit of 1.25 pu [29]. Therefore, there is a need to control both the steady-state

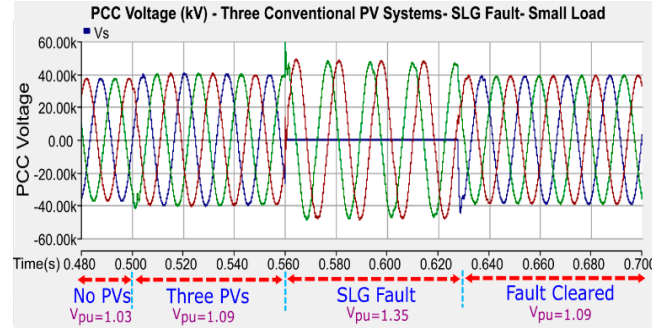


Fig. 7. Performance of three conventional PV systems during small load and Single-Line-to-Ground (SLG) Fault

overvoltage and the TOV. Additional studies reveal that during large load condition the steady-state voltage is 1.01 pu whereas the TOV is 1.23 pu during SLG fault, both of which are within utility specified limits. These studies (although not included in the paper due to space limit) demonstrate that there is no need for either voltage regulation or TOV reduction during heavy loading condition.

### B. Smart PV Inverter PV-STATCOM and Two Conventional PV systems

In this study, instead of using an external STATCOM, the incoming third PV system is equipped with the proposed smart PV inverter PV-STATCOM controller, while the other two PV systems operate as conventional PV systems. The proposed smart inverter controller regulates the PCC voltage in steady-state with the remaining capacity of the inverter and also converts the PV system to Full STATCOM mode during a TOV event. Two different faults, single line-to-ground (SLG) fault and line-to-line-ground (LLG) fault, are considered to demonstrate the performance of the proposed controller.

#### 1) Single Line to Ground (SLG) Fault

Fig. 8 (a)-(h) demonstrate the per-unit value of the PCC voltage ( $V_{pcc,pu}$ ), the three-phase instantaneous PCC voltage ( $v_{pcc}$ ), smart PV system current ( $i_s$ ), output powers ( $P_{PV}$ ,  $Q_{PV}$ ), reactive current ( $I_q$ ) active current ( $I_d$ ), DC link voltage ( $V_{dc}$ ), angular frequency, PLL angle output and TOV flag status, respectively.

$t < 0.5$  sec: The smart PV system is not connected, and hence the real and reactive power of PV system are respectively, zero.

$t = 0.5$  sec: *Three conventional PV system connected:* Due to 21 MW active power generation of PV systems, the PCC voltage increases from 1.04 pu to 1.10 pu which is unacceptable. The DC link voltage is controlled at reference value by controlling active current output. The reactive power is controlled at zero.

$t = 0.54$  sec: *Partial STATCOM mode enabled:* This operating mode for voltage control reduces the voltage to an acceptable range in less than one cycle utilizing the remaining capacity of the inverter. The reactive power output of the inverter reaches 7 Mvar capacitive from zero to maintain the voltage at acceptable range. However, the active power remains at same value since the reactive power control utilizes the remaining capacity of the inverter. The active and reactive

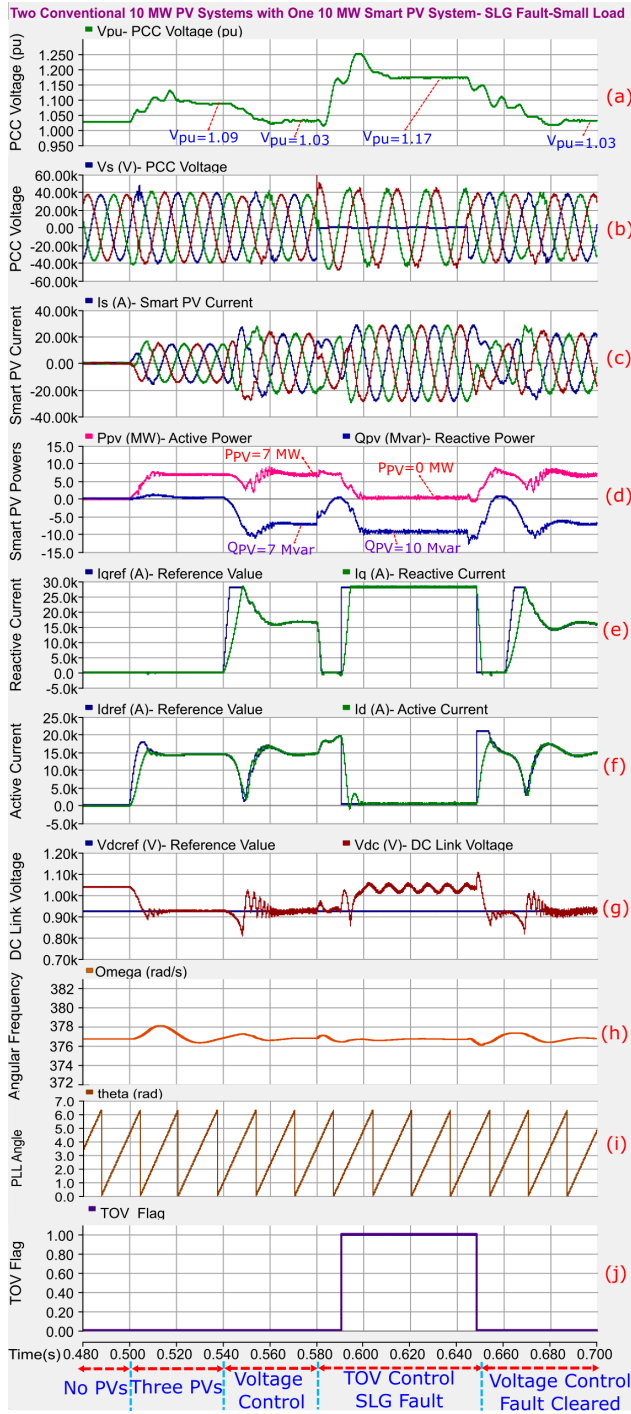


Fig. 8. Performance of the third 10 MW PV system as PV-STATCOM, together with two conventional PV systems, during small load and SLG fault a) PCC voltage (pu) b) PCC voltage c) Smart PV current d) Active and reactive powers e) Reactive current f) Active current g) DC link voltage h) Angular frequency of PCC voltage i) Angle output of PLL j) TOV flag status

currents follow their reference values to satisfy the voltage control objective.

$t=0.58$  sec: *SLG fault initiated*: the SLG fault causes the voltage of phase “A” to fall to zero, whereas the other phase voltages experience TOV. The proposed TOV detection unit detects this TOV event and triggers the TOV flag. Hence, the smart inverter autonomously switches from Partial STATCOM

mode for voltage control to Full STATCOM mode for TOV reduction. In this situation, the controller changes the DC link voltage of the inverter to a value equal to the open circuit voltage of the solar panels (Fig. 8 (g)). It subsequently absorbs reactive power with full capacity of the inverter to reduce the voltages of phase “B” and phase “C”. On comparing with Fig. 8 (a), it is revealed that the proposed smart PV inverter control reduces the PCC voltage from 1.35 pu to 1.23 pu which is below the TOV limit specified in [29]. Fig. 8 (d) illustrates that active power output reaches zero and the entire capacity of the inverter is used for reactive power absorption.

$t=0.63$  sec: *SLG fault cleared*: the fault is cleared and the controller returns to Partial STATCOM mode for voltage control while generating active power. The PCC voltage is controlled to an acceptable level (1.03 pu) by using the remaining capacity of the inverter.

## 2) Line to Line to Ground (LLG) Fault

The performance of the proposed smart inverter controller during an LLG fault is demonstrated in Fig. 9. As in the previous case of SLG fault, the smart PV inverter controls the PCC voltage to its reference value during steady-state.

$t=0.58$  sec: *LLG fault initiated*: the voltages of two phases phase “A” and phase “B” fall to zero and a TOV is caused in phase “C” due to LLG fault. The TOV detection unit triggers the TOV flag and the controller changes its mode from Partial STATCOM mode for voltage control to Full STATCOM mode for TOV reduction. This smart inverter control effectively reduces the TOV in the healthy phase to an acceptable value of 1.22 pu in about a cycle. It is noted that the designed PLL performs in a stable manner both during steady state and during SLG and LLG faults.

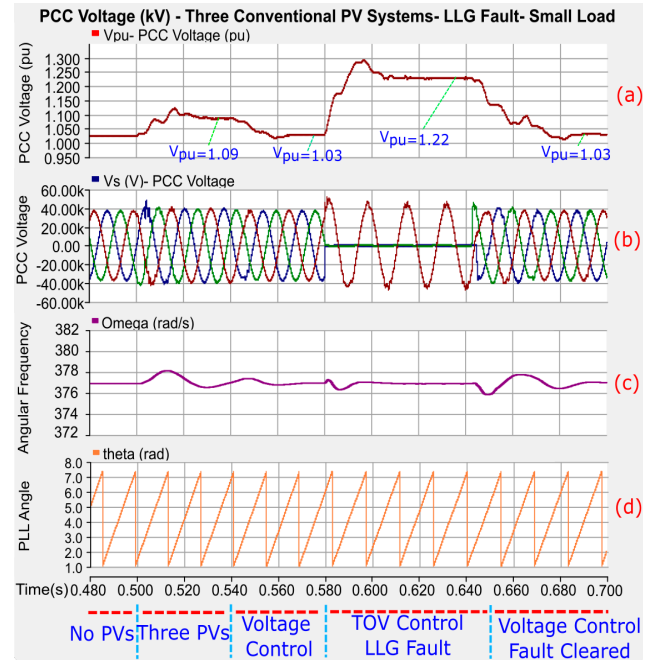


Fig. 9. Performance of one PV system with proposed smart inverter control, together with two conventional PV systems, during small load and LLG fault a) PCC voltage (pu) b) Instantaneous PCC voltage c) Angular frequency of PCC voltage d) Angle output of PLL



## VII. DISCUSSIONS

The proposed smart inverter PV-STATCOM provides TOV mitigation using the full inverter capacity both during night and anytime during the day as needed by the grid. It provides steady state voltage control throughout the night. During daytime, it is assumed in this study that light load conditions do not arise during full noon hours i.e., when the solar system is producing its rated power. Hence there is some remaining inverter capacity available for steady state voltage regulation in Partial STATCOM mode. Under the revised IEEE Standard 1547 - 2018, the PV inverters are also expected to provide reactive power injection and absorption capability of 44% and 25% of nameplate apparent power rating, respectively. This oversizing will further leave room for adequate steady state voltage control in the Partial PV-STATCOM mode. In the worst case, if light load conditions do arise due to a disturbance during noon hours, the solar farm can switch to Full PV-STATCOM mode for voltage control as long as the disturbance lasts. In other words, the proposed control offers the full functionality of a STATCOM for voltage control during day or night.

This proposed novel smart inverter control can therefore potentially eliminate the need for the physical STATCOM, thereby saving an enormous expense for utilities. Table I shows the comparison between different systems. It is noted that the PV-STATCOM control proposed in [27] which was meant to provide only steady state voltage control is unable to mitigate the TOV issue. It is only with the TOV control strategy proposed in this paper, the PV solar farm as PV-STATCOM can suppress TOV effectively. In Table I, the acceptable steady state voltage range is between 0.94 pu and 1.05 pu whereas the TOV limit is 1.25 pu [29]. Due to the lack of space, the results

of STATCOM with and without TOV control [34] have not been demonstrated in this paper.

Table I also presents a cost-comparison of the different options. The PV-STATCOM is 50-100 times cheaper than an equivalent STATCOM for accomplishing the same voltage control functions. This is because only the additional PV-STATCOM control with its associated control and measurement circuitry, and protection needs to be installed on the existing inverters of the PV solar farm. The entire existing electrical (and civil) substation infrastructure of the PV solar farm including the transformers, bus-work, circuit breakers, lines and cables, etc. is utilized for implementing the overall PV-STATCOM. If a new SVC or STATCOM needs to be commissioned, the complete substation needs to be built all over, and new inverter needs to be procured. These costs are clearly avoided with PV-STATCOM.

This paper considers a single equivalent inverter for an entire PV solar farm to demonstrate a new control concept, whereas an actual solar farm may have multiple inverters involving plant controls and communication delays, etc. In such a situation, some PV inverters being utilized as PV-STATCOMs may need to bypass the plant controls and respond rapidly to TOVs in the grid. Such controls are being developed and will be reported in a future paper.

## VIII. CONCLUSIONS

This paper presents an innovative smart PV inverter control as STATCOM, named PV-STATCOM, for controlling the steady state overvoltage and more importantly, mitigation of Temporary Overvoltages (TOV). This novel control in Partial STATCOM mode regulates the steady state over voltage to the desired reference value within one and half cycle. Further, this smart inverter control in Full STATCOM mode successfully reduces the TOV caused during both single line to ground fault and line to line to ground fault to within utility acceptable values within one cycle. The PV-STATCOM thus provides the full function of a STATCOM for voltage control on a 24/7 basis.

For the studied actual distribution system the proposed PV-STATCOM control can help integrate the third 10 MW PV solar farm thereby eliminating the need for the actually installed STATCOM for the same purpose. The proposed PV-STATCOM control is expected to be at least 50 times cheaper than a conventional STATCOM. This control can therefore bring a significant saving for the concerned utility. Such a control can also help in increasing the hosting capacity of PV solar farms on distribution systems which may be restricted due to voltage issues. This control can potentially open a new revenue making opportunity for the solar farms for providing the STATCOM service.

## IX. ACKNOWLEDGMENTS

Dr. Luis Marti, Dr. L. Tang, and Dr. A. Yan are gratefully acknowledged for their feedback and support in this work.

## X. REFERENCES

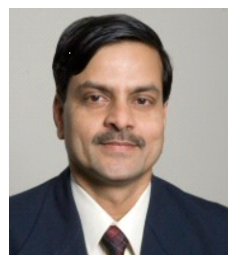
- [1] F. Katiraei and J. R. Aguero, "Solar PV Integration Challenges," in IEEE Power and Energy Magazine, vol. 9, no. 3, pp. 62-71, May-June 2011.

Table I. Comparison of different devices for voltage control

Devices Features	Conven- tional PV System	STATCOM with Voltage Control	STATCOM with Voltage and TOV Controls	PV- STATCOM with Voltage and TOV Controls
Capacity	30 MW 0 Mvar	3.5 Mvar	10 Mvar	10 MW/ 10 Mvar
TOV Magnitude	1.35 pu	1.43 pu	1.24 pu	1.22 pu
Steady State Voltage	1.10 pu	1.02 pu	1.02 pu	1.02 pu
Response Time	----	Half Cycle	Half Cycle	Half Cycle
External Devices	----	Yes	Yes	No
Steady-State Voltage Test	Fail	Pass	Pass	Pass
TOV Test	Fail	Fail	Pass	Pass
Cost	----	~\$5 Millions	~\$ 8 Millions	~\$ 0.2 Million

- [2] Obi, Manasseh, and Robert Bass. "Trends and challenges of grid-connected photovoltaic systems—A review." *Renewable and Sustainable Energy Reviews* 58 (2016): 1082-1094.
- [3] D. Cheng, B. A. Mather, R. Seguin, J. Hambrick, and R. P. Broadwater, "Photovoltaic (PV) impact assessment for very high penetration levels," *IEEE Journal of Photovoltaics*, vol. 6, pp. 295-300, 2016.
- [4] "High-Penetration PV Integration Handbook for Distribution Engineers", Technical Report NREL/TP-5D00-63114 January 2016
- [5] R. J. Bravo, R. Salas, T. Bialek, and C. Sun, "Distributed energy resources challenges for utilities," *Proc. 2015 IEEE 42nd Photovoltaic Specialist Conference, PVSC 2015*, 2015.
- [6] Jeff Smith and Matt Rylander, "PV Hosting Capacity on Distribution Feeders", *Proc. 2014 IEEE PES GM, Washington, USA*, 2014
- [7] SJ Steffel, PR Caroselli, AM Dinkel, JQ Liu, RN Sackey, and NR Vadhar, "Integrating solar generation on the electric distribution grid," *IEEE Transactions on Smart Grid*, vol. 3, pp. 878-886, 2012
- [8] Y. Kabasawa, T. Noda, K. Fukushima and K. Nemoto, "Consumer voltage regulation using coordinated control of distributed static synchronous compensators - STATCOMs," in *Proc. 2012 3rd IEEE PES Innovative Smart Grid Technologies Europe*, pp. 1-7.
- [9] N. G. Hingorani and L. Gyugyi, *Understanding FACTS*, New York: IEEE-Wiley, 1999.
- [10] "System Impact Assessment Report – Grand Renewable Energy Park Project" Independent Electricity System Operator (IESO) Report No. CAA ID 2010-399, May 2011
- [11] D. Iio, K. Sakakibara, Y. Yokomizu, T. Matsumura and N. Izuwara, "Distribution voltage rise at dense photovoltaic generation area and its suppression by SVC," *Electrical Engineering in Japan*, vol. 166, no.2, pp. 47-53, 2009.
- [12] G. E. M. Aly, A. El-Zeftawy, A. El-Hefanwy and S. A. Eraky, "Reactive power control on residential utility-interactive PV power systems," *Electr. Power Syst. Res.*, vol. 51, no. 3, pp. 187-199, 1999.
- [13] N. K. Roy, H. R. Pota, A. Mahmud and M. J. Hossain, "D-STATCOM control in distribution networks with composite loads to ensure grid code compatible performance of photovoltaic generators," in *Proc. 2013 IEEE 8th Conf. on Industrial Electronics and Applications*, pp. 55-60.
- [14] [https://library.e.abb.com/public/9ae411b2ed304cbb37115159e81fb5d/9AAK10103A2230\\_PV-Cluster\\_STATCOM-CS-LR.pdf](https://library.e.abb.com/public/9ae411b2ed304cbb37115159e81fb5d/9AAK10103A2230_PV-Cluster_STATCOM-CS-LR.pdf)
- [15] <http://www.abb.pl/cawp/seitp202/c3a70ee0924b6062c12580ec00529aa0.aspx>
- [16] L. Tang, A. Yan, A. Narang, M. Ali, and L. Marti, "Mitigation for Connecting Distributed Generators beyond Power Distance Limitation", paper 436, *Proc. 2014 CIGRE Canada Conference, Toronto, Sep. 2014*.
- [17] Yi Zhang, C. Mensah-Bonsu, P. Walke, S. Arora and J. Pierce, "Transient over-voltages in high voltage grid-connected PV solar interconnection", in *Proc. 2010 IEEE Power & Energy Society General Meeting*, pp. 1-6.
- [18] J. W. Smith, W. Sunderman, R. Dugan and B. Seal, "Smart inverter volt/var control functions for high penetration of PV on distribution systems," in *Proc. IEEE PSCE*, 2011, pp. 1-6.
- [19] "Common Functions for Smart Inverters, Version 3", EPRI Palo Alto, CA, Report No. 3002002233, Feb. 2014
- [20] B. Mather, "NREL/SCE High-Penetration PV Integration Project: Report on Field Demonstration of Advanced Inverter Functionality in Fontana, CA", NREL Report NREL/TP-5D00-62483, 2014.
- [21] M. Morjaria, D. Anichkov, V. Chadliev, and S. Soni, "A Grid-Friendly Plant", *IEEE Power and Energy Magazine*, May-June 2014, pp. 87-95
- [22] IEEE 1547-2018, IEEE Standard for Interconnecting Distributed Resources with Electric Power Systems, IEEE Standards Association, 2018
- [23] R. K. Varma, V. Khadkikar, and R. Seethapathy, "Nighttime application of PV solar farm as STATCOM to regulate grid voltage," *IEEE Trans. Energy Conversion (Letters)*, vol. 24-4, pp. 983-985, 2009
- [24] Rajiv K. Varma, V. Khadkikar and S. A. Rahman, "Utilization of Distributed Generator Inverters as STATCOM" PCT Patent application PCT/CA2010/001419 filed on 15 September, 2010.
- [25] R. K. Varma, S. A. Rahman, M. A.C., R. Seethapathy and T. Vanderheide, "Novel Nighttime Application of PV Solar Farms as STATCOM (PV-STATCOM)", *Proc. IEEE PES GM*, 2012
- [26] R. K. Varma, S. A. Rahman, and T. Vanderheide, "Novel Control of PV Solar Farm as STATCOM (PV-STATCOM) for Enhancing Grid Power Transmission Limits During Night and Day", *IEEE Trans. on Power Delivery*, Vol. 30, No. 2, pp 755-763, April 2015
- [27] Rajiv K. Varma and Ehsan Siavashi, "PV-STATCOM – A New Smart Inverter for Voltage Control in Distribution Systems", *IEEE Transactions on Sustainable Energy*, IEEE Xplore Early Access, Digital Object Identifier: 10.1109/TSTE.2018.2808601
- [28] R. K. Varma, "Multivariable Modulator Controller for Power Generation Facility", PCT Application (PCT/CA2014/051174) filed Dec. 6, 2014
- [29] Hydro One Inc. (2013). Distributed Generation Technical Interconnection Requirements- Interconnections at Voltages 50kV and Below (Rev. 3 ed.)
- [30] A. Yazdani, A. R. Di Fazio, H. Ghoddami, et al., "Modeling guidelines and a benchmark for power system simulation studies of three-phase single-stage photovoltaic systems," *IEEE Transactions Power Delivery*, vol. 26, no. 2, pp. 1247-1264, 2011.
- [31] M. Liserre, F. Blaabjerg, and S. Hansen, "Design and control of an LCL-filter-based three-phase active rectifier," *Industry Applications*, *IEEE Transactions on*, vol. 41, no. 5, pp. 1281-1291, 2005.
- [32] A. Yazdani and R. Iravani, *Voltage-sourced converters in power systems: modeling, control, and applications*. John Wiley & Sons, 2010.
- [33] W. Leonhard, *Control of Electrical Drives*. Springer Science & Business Media, 2001.
- [34] E. M. Siavashi, "Smart PV inverter control for distribution systems," in *Electronic Thesis and Dissertation Repository*. 3065. <https://ir.lib.uwo.ca/etd/3065>, 2015.
- [35] P. P. Dash and A. Yazdani, "A mathematical model and performance evaluation for a single-stage grid-connected photovoltaic (PV) system," *International Journal of Emerging Electric Power Systems*, vol. 9, no. 6, 2008.

## XI. BIOGRAPHY



**Rajiv K. Varma** (M'90-SM'09) obtained B.Tech. and Ph.D. degrees in Electrical Engineering from Indian Institute of Technology (IIT), Kanpur, India, in 1980 and 1988, respectively. He is currently a Professor with The University of Western Ontario, London, ON, Canada. He was the Hydro One Chair in power systems engineering with The University of Western Ontario from 2012 to 2015. Prior to this position, he was a faculty member in the Electrical Engineering Department at IIT Kanpur, India, from 1989-2001. He has co-authored an IEEE Press/Wiley book on Thyristor Based FACTS Controllers. He has co-delivered several Tutorials (IEEE sponsored), Courses and Workshops on Smart Inverters, FACTS, SVC and HVDC in different countries. His research interests include FACTS, power systems stability, and grid integration of photovoltaic solar and wind power systems. He is active on several IEEE Working Groups. He is presently the Vice Chair of the IEEE "HVDC and FACTS Subcommittee" and Chair of IEEE Working Group 15.05.17 on "HVDC and FACTS Bibliography" since 2004.



**Ehsan M. Siavashi** (M'11) Ehsan M. Siavashi obtained B.Sc. degree in Electrical Engineering from K.N. Toosi University of Technology and M.Sc. degree in Power Electronics from University of Tehran, Tehran, Iran in 2007 and 2010, respectively. Also, he received the Ph.D. degree in power systems engineering from Western University, London, ON, Canada, in 2015. Currently, he is a power systems studies engineer at Powertech Labs Inc., British Columbia, Canada. Prior to this position, he was postdoctoral fellow at Western University from 2015 to 2017. His main areas of interests include FACTS, microgrids, power electronics, photovoltaic solar systems and power quality